

## **Terahertz microfluidic sensor based on a parallel-plate waveguide resonant cavity**

Rajind Mendis, Victoria Astley, Jingbo Liu, and Daniel M. Mittleman

Citation: [Applied Physics Letters](#) **95**, 1711113 (2009); doi: 10.1063/1.3251079

View online: <http://dx.doi.org/10.1063/1.3251079>

View Table of Contents: <http://scitation.aip.org/content/aip/journal/apl/95/17?ver=pdfcov>

Published by the [AIP Publishing](#)

---

### **Articles you may be interested in**

[Surface sensitive microfluidic optomechanical ring resonator sensors](#)

Appl. Phys. Lett. **105**, 191101 (2014); 10.1063/1.4901067

[Terahertz multichannel microfluidic sensor based on parallel-plate waveguide resonant cavities](#)

Appl. Phys. Lett. **100**, 231108 (2012); 10.1063/1.4724204

[Coupled-resonator optical waveguides for biochemical sensing of nanoliter volumes of analyte in the terahertz region](#)

Appl. Phys. Lett. **87**, 241119 (2005); 10.1063/1.2140479

[Refractometric sensors based on microsphere resonators](#)

Appl. Phys. Lett. **87**, 201107 (2005); 10.1063/1.2132076

[Prism coupled terahertz waveguide sensor](#)

Appl. Phys. Lett. **86**, 211119 (2005); 10.1063/1.1940127

---

The image shows the cover of the journal Applied Physics Reviews. It features a white background with a blue and orange design. The title 'AIP Applied Physics Reviews' is at the top. Below it is a diagram of a device structure. The AIP logo is at the bottom left.

## **NEW Special Topic Sections**

**NOW ONLINE**  
Lithium Niobate Properties and Applications:  
Reviews of Emerging Trends

**AIP** | Applied Physics Reviews

# Terahertz microfluidic sensor based on a parallel-plate waveguide resonant cavity

Rajind Mendis,<sup>a)</sup> Victoria Astley, Jingbo Liu, and Daniel M. Mittleman

Department of Electrical and Computer Engineering, Rice University, MS-366, 6100 Main Street, Houston, Texas 77005, USA

(Received 24 August 2009; accepted 29 September 2009; published online 30 October 2009)

We describe a terahertz optical resonator that is ideally suited for highly sensitive and noninvasive refractive-index monitoring. The resonator is formed by machining a rectangular groove into one plate of a parallel-plate waveguide, and is excited using the lowest-order transverse-electric ( $TE_1$ ) waveguide mode. Since the resonator can act as a channel for fluid flow, it can be easily integrated into a microfluidics platform for real-time monitoring. Using this resonator with only a few microliters of liquid, we demonstrate a refractive-index sensitivity of  $3.7 \times 10^5$  nm/refractive-index-unit, the highest ever reported in any frequency range. © 2009 American Institute of Physics. [doi:10.1063/1.3251079]

Ultrasensitive optical sensing often relies on engineered structures with resonant responses. The characteristic frequency of these resonances can be a very sensitive measure of the refractive index of the surrounding medium. This sensing strategy has been the focus of considerable research in the terahertz (THz) region of the spectrum.<sup>1</sup> For example, planar integrated waveguide resonators<sup>2</sup> and asymmetric split ring arrays<sup>3</sup> have been used to detect DNA hybridization and denaturing. Coupled THz resonators<sup>4</sup> and resonant metal meshes<sup>5</sup> have been studied for biochemical sensing. Planar structures have even been used to study nanometer-thick films of material, which demonstrates their exquisite sensitivity.<sup>6,7</sup> However, a crucial limitation with most of these examples is their planar or open geometry, which is not compatible with flow monitoring as is required in microfluidics or on-line process applications.<sup>8</sup> Additionally, the resolution of this type of sensing strategy is limited by the intrinsic linewidth of the resonant line, since sublinewidth shifts are difficult to detect.<sup>9–13</sup>

Here, we describe a THz resonator, integrated with a parallel-plate waveguide (PPWG), which addresses these issues. It exhibits among the narrowest linewidths reported for an artificial resonance in the THz range. Moreover, since the resonator can also act as a channel for fluid flow, it can be easily integrated into a microfluidic platform for real-time monitoring.<sup>14,15</sup> Using this resonator, we demonstrate a refractive-index sensitivity of  $3.7 \times 10^5$  nm/RIU (refractive-index-unit), the highest ever reported in any frequency range.

Recently, we introduced the use of the rarely exploited lowest-order transverse-electric ( $TE_1$ ) mode of the PPWG for enabling applications in THz photonics.<sup>16,17</sup> Here, we describe one such application: the excitation of a very simple, practical, and highly effective resonant cavity integrated into a PPWG. This cavity cannot be excited by the far more commonly employed transverse-electromagnetic (TEM) mode of the waveguide.<sup>18</sup> As a result, although the PPWG geometry has been extensively investigated for almost a century, this coupled-resonant-cavity has not been studied before. In this work, we demonstrate the use of this PPWG-cavity system

as a prototype configuration for process monitoring and microfluidic sensing, which can be employed to determine the refractive index of microliter liquid volumes in the THz regime.

The device geometry is illustrated in Fig. 1. The PPWG, consisting of two polished aluminum plates, is assembled

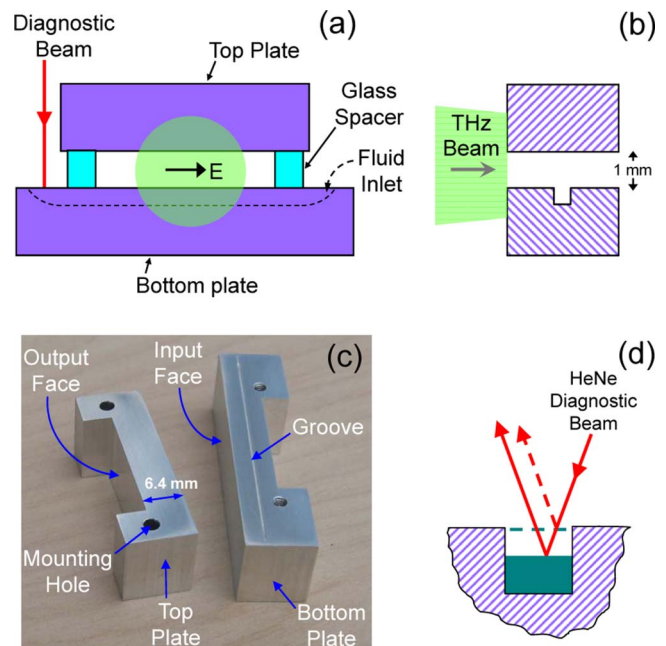


FIG. 1. (Color online) (a) Input face of the assembled PPWG (not to scale). The dashed line on the bottom plate shows the longitudinal profile of the groove cut into the lower plate, forming the resonant cavity. This groove, situated halfway between the input and output faces of the waveguide, has a nearly rectangular cross-section with a width of  $472 \mu\text{m}$  and a depth of  $412 \mu\text{m}$ , as measured by wax molding. One uncovered end of the groove is used as the fluid inlet (right side) and the other end is used for the optical diagnostic beam. The circular (green) spot indicates the input THz beam, which is smaller than the width of the plates. The electric field is polarized parallel to the plate surfaces to excite the  $TE_1$  mode. The glass spacers maintain a 1 mm separation between the plates. (b) Axial cross-section of the device along the direction of propagation showing the transverse profile of the groove on the bottom plate. The propagation length of the waveguide is 6.4 mm. (c) Photograph of the disassembled waveguide, where the inside surfaces are facing up. (d) Sketch of the optical diagnostic beam used to track the fluid level inside the groove.

<sup>a)</sup>Electronic mail: rajind@rice.edu.

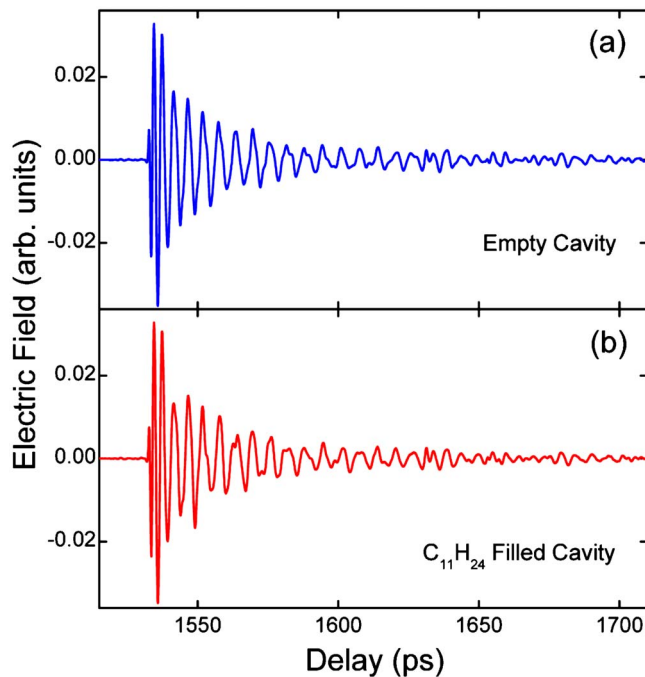


FIG. 2. (Color online) THz time-domain waveforms after propagation through the waveguide with (a) an empty cavity and (b) a filled cavity. Here, the cavity is completely filled with liquid undecane ( $C_{11}H_{24}$ ). Each waveform is an average of 10 000 scans of a rapid delay line, requiring less than 2 min of averaging.

with glass spacers to provide a plate separation of 1 mm. A groove machined into the lower plate forms a resonant cavity for the propagating electromagnetic wave and also act as a channel for containing liquids. The groove slopes up at both ends in order to contain the liquid under study. (One could easily imagine that it could form one leg of a contained microflow system). We use a focused HeNe laser beam to monitor the filling of the groove with fluid, which we accomplish manually using a precision syringe. The total volume of liquid required to fill the groove is  $\sim 8 \mu\text{l}$ .

We characterize the PPWG-cavity system using a commercial THz-TDS (time-domain-spectroscopy) system producing single-cycle THz pulses. The THz beam is coupled into and out of the PPWG using conventional quasi-optics, polarized parallel to the plates in order to excite the single- $TE_1$  mode of the waveguide.<sup>16,17</sup> As shown in Fig. 2(a), the output pulse (with an empty cavity) is strongly chirped and broadened due to group velocity dispersion, as expected. The amplitude spectrum (blue), shown in Fig. 3, exhibits a marked low-frequency cutoff at 0.15 THz, as determined by the 1 mm plate separation. We also observe a strong and narrow dip in the spectrum at 0.293 THz, caused by the (empty) resonant cavity.

In a second set of experiments, we repeat the transmission measurements, this time with the cavity filled with a series of liquids. For our test liquids, we choose *N*-alkanes, a homologous series of linear chain hydrocarbons with well-characterized (and nearly frequency-independent) refractive indices in the THz range. We use nine different chain lengths ranging from  $C_8H_{18}$  (octane) up to  $C_{16}H_{34}$  (hexadecane), all with purities of 98% or better. For each liquid sample, we take measurements for both the empty and filled cavity, without disturbing the position of the device with respect to the THz beam. A typical time-domain waveform [for undecane

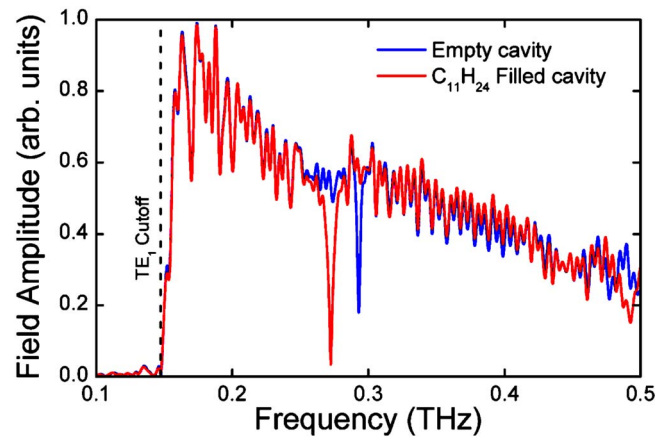


FIG. 3. (Color online) Amplitude spectra corresponding to the waveforms shown in Figs. 2(a) and 2(b), obtained by Fourier transforming the original 320 ps time signals zero-padded to 5120 ps. The redshift in the resonance dip due to the dielectric filling is clearly evident. Both spectra show a waveguide cutoff at 0.15 THz due to the 1 mm plate separation.

( $C_{11}H_{24}$ )] is shown in Fig. 2(b), with the corresponding amplitude spectrum (red) in Fig. 3. Clearly, the resonant dip has shifted to a lower frequency because of the dielectric filling.

Since the resonance dips for the sample and reference measurements are spectrally well separated, we can take the square of the ratio, and the square of the inverse-ratio, to derive the power transmission spectra of the empty and filled cavities, respectively. This analytical technique eliminates any envelope ripples in the spectra that result from artifacts in our THz-TDS system, and permits an accurate line shape analysis. These two spectra are plotted in Fig. 4 by the black dots, along with fits to Lorentzian line shapes. The fit for the empty cavity (blue) indicates a resonance frequency of 0.293 THz and a 3-dB linewidth of 3 GHz, whereas the fit for the filled cavity (red) indicates a linewidth of 6 GHz and an extinction coefficient of almost 30 dB. Although the quality factor ( $Q \sim 98$ ) is not the highest measured for an artificial structure in the THz range,<sup>10</sup> the 3 GHz linewidth is the

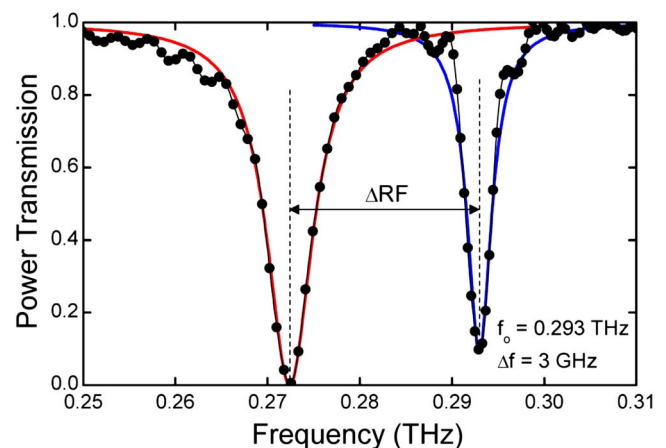


FIG. 4. (Color online) Power transmission (dots) in the vicinity of the resonance dips, derived by taking the square of the ratio, and the inverse-ratio, of the spectra in Fig. 3. These are fit to Lorentzian line shapes (blue and red solid curves). These fits indicate a resonant frequency of 0.293 THz and a linewidth of 3 GHz for the empty cavity, and a linewidth of 6 GHz and an extinction coefficient of 30 dB for the filled cavity. This result is used to derive the resonant-frequency shift ( $\Delta RF$ ) for each of the different liquids studied.



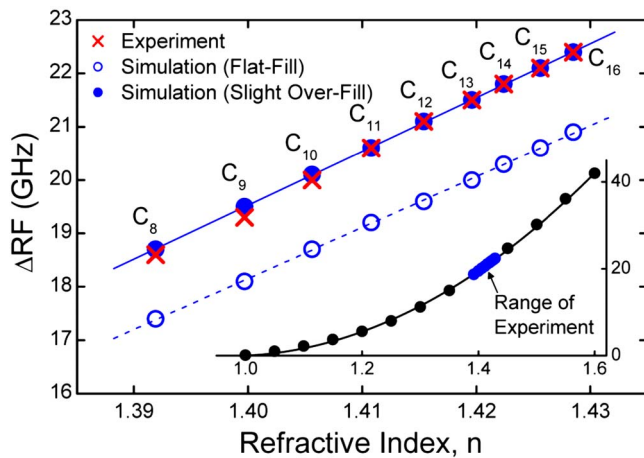


FIG. 5. (Color online) Experimental (red x-marks) and simulated (blue dots and open circles) resonant-frequency shift ( $\Delta RF$ ) plotted against the refractive index ( $n$ ) for a series of high-purity linear  $N$ -alkanes, ranging from octane (carbon number=8) to hexadecane (carbon number=16). The solid and dashed lines denote least-squares linear fits to the simulations. The blue open circles correspond to simulations in which the resonant cavity is filled completely with a flat fill. For the blue dots, the simulations are modified to include a small convex meniscus on the filled cavity with a height of  $9\ \mu\text{m}$ . The inset shows the simulated values (black dots) for the slightly overfilled cavity over a much wider range of  $n$  values, revealing a nonlinear dependence. The solid black curve through these dots is a quadratic fit ( $106.25n^2 - 206.25n + 100$ ), which shows excellent agreement.

narrowest ever directly measured for a PPWG-based resonant cavity,<sup>17</sup> and is among the narrowest measured for any resonator in the THz range.<sup>9–13</sup> The increase in linewidth for the filled cavity can be attributed to the higher refractive index of the fluid, and also due to its non-negligible absorption. The dramatic redshift is a signature of the refractive index of the material inside the resonator, and demonstrates how this system can be used as a highly sensitive refractive-index sensor.

To investigate this possibility, we determine the sensitivity of the sensor to shifts in the refractive index of the liquid filling the cavity. In Fig. 5, we plot the measured shifts in the resonant frequency ( $\Delta RF$ ) versus the refractive indices of the various  $N$ -alkanes (red x-marks), which have been determined from independent studies. For each of the  $N$ -alkane samples,  $\Delta RF$  is determined using the reference and sample transmission spectra as shown in Fig. 4. We compare these results to finite-element-method simulations, which include the filling of the cavity by a nonabsorbing dielectric. These simulated values (open blue circles) assume that the groove is filled perfectly to the top with a flat fill. A consistent  $\sim 1$  GHz shift between these simulations and the measured data suggest a slight systematic correction is required. This takes the form of a slight overfilling of the groove using a convex meniscus of  $9\ \mu\text{m}$  radius in the simulations. This value of the meniscus curvature is chosen so that the simulated value of  $\Delta RF$  matches the experimental value for undecane ( $C_{11}H_{24}$ ). We then use this meniscus-curvature value for all of the subsequent simulations. These results (blue dots) match the experimental results extremely well. We note that the data points indicate a linear fit over this range of refractive indices. The inset shows the results of simulations (black dots) over a much broader range of refractive-index values, ranging from 1.0 to 1.6. Here, a global nonlinear dependence of  $\Delta RF$  on  $n$  becomes clear. A quadratic fit (solid

curve) gives almost perfect agreement over this entire range of index values.

To compare the sensitivity of our device to that of other devices reported in the literature for optical refractive-index sensing, we differentiate the quadratic fit to obtain  $\Delta f/\Delta n = 91.25\ \text{GHz}/\text{RIU}$  within our experimental range (near  $n \sim 1.4$ ). Converting frequency into wavelength, we obtain the sensitivity in conventional units as  $\Delta\lambda/\Delta n = 3.7 \times 10^5\ \text{nm}/\text{RIU}$ . This value is more than an order of magnitude higher than the highest (theoretical) value reported in the THz regime for a photonic-crystal-based sensor,<sup>4</sup> and almost an order of magnitude higher than the highest values reported in the optical regime for a surface-plasmon-based sensor.<sup>19–21</sup>

In conclusion, we have experimentally demonstrated a highly sensitive fluid refractive-index sensor based on a simple resonant cavity integrated with a PPWG that can be efficiently excited via the  $TE_1$  mode. The linewidth of the empty cavity is among the narrowest measured in the THz range, while the refractive-index sensitivity is the highest ever reported in any frequency regime. This noninvasive sensor can easily be used in conjunction with fluid process monitoring or microfluidic lab-on-a-chip configurations. In addition, the resonant frequency is easy to engineer, simply by changing the dimensions of the machined groove. The simplicity of the design also affords a great deal of flexibility in the implementation, including the possibility of multiple parallel and independent sensors in a single waveguide.

We are grateful to Jonathan Laib for the THz refractive-index measurements of the alkane samples. This work was supported in part by the R. A. Welch Foundation, the National Science Foundation, and the Air Force Office of Scientific Research through the CONTACT program.

- <sup>1</sup>C. K. Tiang, J. Cunningham, C. Wood, I. C. Hunter, and A. G. Davies, *J. Appl. Phys.* **100**, 066105 (2006).
- <sup>2</sup>M. Nagel, P. H. Bolivar, M. Brucherseifer, H. Kurz, A. Bosserhoff, and R. Buttner, *Appl. Phys. Lett.* **80**, 154 (2002).
- <sup>3</sup>C. Debus and P. H. Bolivar, *Appl. Phys. Lett.* **91**, 184102 (2007).
- <sup>4</sup>H. Kurt and D. S. Citrin, *Appl. Phys. Lett.* **87**, 241119 (2005).
- <sup>5</sup>H. Yoshida, Y. Ogawa, Y. Kawai, S. Hayashi, A. Hayashi, C. Otani, E. Kato, F. Miyamaru, and K. Kawase, *Appl. Phys. Lett.* **91**, 253901 (2007).
- <sup>6</sup>Y. Sun, X. Xia, H. Feng, H. Yang, C. Gu, and L. Wang, *Appl. Phys. Lett.* **92**, 221101 (2008).
- <sup>7</sup>J. F. O'Hara, R. Singh, I. Brener, E. Smirnova, J. Han, A. J. Taylor, and W. Zhang, *Opt. Express* **16**, 1786 (2008).
- <sup>8</sup>B. Kuswandi, J. Nuriman, J. Huskens, and W. Verboom, *Anal. Chim. Acta* **601**, 141 (2007).
- <sup>9</sup>A. L. Bingham and D. Grischkowsky, *Opt. Lett.* **33**, 348 (2008).
- <sup>10</sup>C. M. Yee and M. S. Sherwin, *Appl. Phys. Lett.* **94**, 154104 (2009).
- <sup>11</sup>S. S. Harsha, N. Laman, and D. Grischkowsky, *Appl. Phys. Lett.* **94**, 091118 (2009).
- <sup>12</sup>P. A. George, C. Manolatu, F. Rana, A. L. Bingham, and D. Grischkowsky, *Appl. Phys. Lett.* **91**, 191122 (2007).
- <sup>13</sup>X. Lu and W. Zhang, *Appl. Phys. Lett.* **94**, 181106 (2009).
- <sup>14</sup>T. Kiwa, S. Oka, J. Kondo, I. Kawayama, H. Yamada, M. Tonouchi, and K. Tsukada, *Jpn. J. Appl. Phys., Part 2* **46**, L1052 (2007).
- <sup>15</sup>P. A. George, W. Hui, F. Rana, B. G. Hawkins, A. E. Smith, and B. J. Kirby, *Opt. Express* **16**, 1577 (2008).
- <sup>16</sup>R. Mendis and D. M. Mittleman, *J. Opt. Soc. Am. B* **26**, A6 (2009).
- <sup>17</sup>R. Mendis and D. M. Mittleman, *Opt. Express* **17**, 14839 (2009).
- <sup>18</sup>R. Mendis and D. Grischkowsky, *Opt. Lett.* **26**, 846 (2001).
- <sup>19</sup>R. Slavik and J. Homola, *Sens. Actuators B* **123**, 10 (2007).
- <sup>20</sup>Q. Liu and K. S. Chang, *Opt. Express* **17**, 7933 (2009).
- <sup>21</sup>J. Henzie, M. H. Lee, and T. W. Odom, *Nat. Nanotechnol.* **2**, 549 (2007).